Shape-from-Template in Flatland

Mathias GALLARDO Daniel PIZARRO Adrien BARTOLI Toby COLLINS

ALCoV-ISIT, UMR6284 CNRS / Université d'Auvergne, Clermont-Ferrand
Corresponding author: Mathias Gallardo (Mathias.Gallardo@gmail.com)

Abstract

Shape-from-Template (SfT) is the problem of inferring the shape of a deformable object as observed in an image using a shape template. We call 2DSfT the 'usual' instance of SfT where the shape is a surface embedded in 3D and the image a 2D projection. We introduce 1DSfT, a novel instance of SfT where the shape is a curve embedded in 2D and the image a 1D projection. We focus on isometric deformations, for which 2DSfT is a well-posed problem, and admits an analytical local solution which may be used to initialize nonconvex refinement. Through a complete theoretical study of 1DSfT with perspective projection, we show that it is related to 2DSfT, but may have very different properties: (i) 1DSfT cannot be exactly solved locally and (ii) 1DSfT cannot be solved uniquely, as it has a discrete amount of at least two solutions. We then propose two convex initialization algorithms, a local analytical one based on infinitesimal planarity and a global one based on inextensibility. We show how nonconvex refinement can be implemented where, contrarily to current 2DSfT methods, one may enforce isometry exactly using a novel angle-based parameterization. Finally, our method is tested with simulated and real data.

1. Introduction

The 1886 novella Flatland [4] describes a 2D world where inhabitants are portrayed by polygons. In Flatland, the social status of a person is determined by its polygon's regularity and number of sides. At the time Flatland was created, a very refined skill was the "Art of Sight Recognition". It was practiced by the highest classes to recognize the social class of others. Colors were forbidden since lower classes could have used them to impersonate noble Polygons. We think that the situation in Flatland has now evolved. Social differences fadded away, as the ancient "Art of Sight Recognition" has been popularized via the use of color and perspective perception. However, the following question has been left unanswered: can a Flatlander recover a curve from its 1D projection matched to a 1D template? We name this problem 1D Shape-from-Template (SfT), as it resembles a problem known as SfT in Mankind's literature, which we here dub 2DSfT for the sake of clarity. 2DSfT involves a 2D image of a 2D surface embedded in 3D, and whose shape is to be reconstructed. The problem involves data constraints provided by the image and a prior on the surface's deformation. The most studied deformation prior is isometry [6, 14, 8], but other models such as conformity [6] and linear elasticity [12] were also studied. Isometric deformations work well for some thin materials such as cloth and paper. Importantly, isometric 2DSfT is a well-posed problem [6].

We introduce 1DSfT and focus on the isometric deformation prior. For 1DSfT this means that the length between any two points of the curve to be reconstructed has been preserved by the deformation. We assume that the 1D template was matched to the 1D image, and that this is conveyed by a smooth 1D warp function, or just *warp*. This is the analogous of the 2D keypoint matches or 2D warp used in 2DSfT [5]. Whether in 1D or 2D, the isometric deformation is not a convex constraint. Existing 2DSfT methods fall in three categories: *(i)* local analytical solutions, *(ii)* convex relaxations and *(iii)* nonconvex refinements. An initial solution obtained by a method in *(i)* or *(ii)* is usually used to initialize a method in *(iii)*. In *(i)* the depth and surface's normal are inferred, independently for each surface point, from the warp and its first-order derivatives. In *(ii)* isometry is relaxed to inextensibility, which is an upper bound on the local surface's extension, and is a convex constraint. In *(iii)* a given solution is refined iteratively by minimizing a weighted combination of the reprojection error and the deformation's un-isometricity. At first sight, it seems that 1DSfT can be directly solved by the literature's results in 2DSfT. It may even look like 1DSfT is an easier problem for one dimension was dropped compared to 2DSfT. While this is true in some respects, this is not in others, as a deeper investigation of the problem reveals. Making a long story short, category *(i)* breaks down in 1DSfT, category *(ii)* is applicable about similarly, and category *(iii)* may be imple-

mented in a better way than in 2DSfT. Maybe more importantly, 1DSfT is not well-posed, as it admits M solutions, with $1 < M < \infty$.

We first give a differential model of 1DSfT, from which we first establish the *non-local solvability* of 1DSfT. Local solvability was established at first-order in 2DSfT; we show that non-local solvability holds at *any order* in 1DSfT. In other words, differenting the 1DSfT equations does not allow one to overcome the growing number of local unknowns. Our analysis also reveals the presence of what we call *critical points*. At these points, the curve's normal is colinear with the line of sight, and depth can then be solved locally. Importantly, the number of solutions M can be shown to be $M \leq 2^{N+1}$, with N the number of critical points. We then propose two approximate initialization algorithms. First, even if 1DSfT is not locally solvable exactly, we show how a locally affine approximation of the curve facilitates local solvability. This leads to a local approximate algorithm, opening an unexplored subcategory in *(i)*. Second, we show how the inextensibility relaxation used with the Maximum Depth Heuristic, which characterizes category *(ii)*, may be directly used. We show how to find the critical points from the warp and to infer the M possible solutions. This involves a nonconvex refinement process, forming an algorithm of category *(iii)*. We show that isometry may be enforced exactly by using an angle-based shape parameterization. This simple parameterization may inspire new research in 2DSfT, where isometry has so far been enforced approximately using a simple penalty in the cost function [7]. This is important, as this solves the problem of choosing the weight combining data and prior in 2DSfT. Finally, we show results on simulated and real data.

Notation. We use Greek letters for functions (*e.g.* φ), bold for vectors (*e.g.* $\mathbf{Q}$) and hats for estimates (*e.g.* $\hat{\mathbf{Q}}$). The first and second derivatives of a function are written with primes (*e.g.* φ'_y and φ''_y). The vector two-norm is denoted $\|.\|_2$. Homogeneous coordinates are written with a bar, for instance $\bar{\eta} = \begin{pmatrix} \eta & 1 \end{pmatrix}^\top$.

2. State of the Art

SfT has been extensively studied for a broad variety of deformation constraints that we can divide in *statistics-based* and *physics-based* methods. Statistics-based methods [10, 14, 9] learn the space of deformations from data. These models are specially effective in low-dimensional spaces of deformations, for instance face gestures. On the contrary, physics-based methods [6, 14, 12] allow an infinite-dimensional space of deformations while using mathematical models inspired in physical laws. The isometric model belongs to this category but other deformation models have been studied such as the conformal [6] model or the slinear elastic model [12]. The isometric model has attracted most of the attention [6, 14, 13]. Isometry is an accurate model for many real object deformations but, more importantly, it makes 2DSfT a well-posed problem [6].

Despite their simplicity, isometric constraints are non-convex and may lead to complex computational solutions. Methods in category *(i)* solve locally a system of non-linear PDEs [6, 8]. They are very fast but they do not ensure isometry in the presence of noise. Methods in *(ii)* relax the non-convex isometric constraints using the so-called Maximum Depth Heuristic (MDH) [13]. The idea is to maximize the surface depth so that the Euclidean distance between every pair of points is upper bounded by its known geodesic distance. They are accurate but fail if the perspective is not strong. Finally, methods in *(iii)* optimize a statistically optimal cost but require iterative non-convex optimization [7]. They need an accurate initialization, usually provided by methods from either *(i)* or *(ii)*.

To sum up, existing methods for isometric 2DSfT solve a well-posed problem, which locally involves 3 constraints and 3 unknowns [6]. 1DSfT turns out to be more difficult in some respects since the number of local isometric constraints drops from 3 to 1 while the number of unknowns drops only from 3 to 2.

3. Modeling

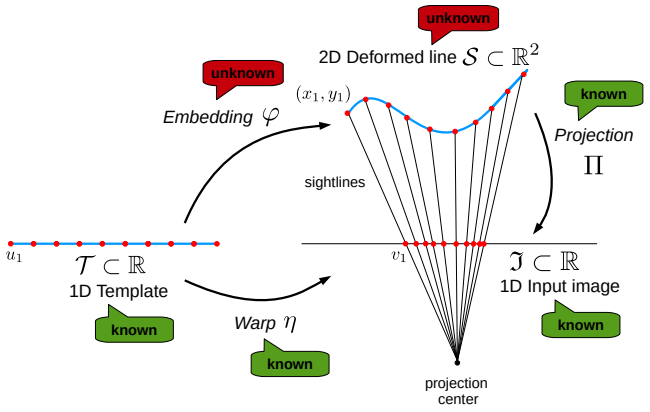

Figure 1. General modeling of 1DSfT, the problem of monocular template-based 2D reconstruction of a deformed curve.

Our modeling is shown in figure 1. It is inspired from [6], where 2DSfT was proposed for 2D images and surfaces embedded in 3D. In 1DSfT, the known template is 1D and we write it as $\mathcal{T} \subset \mathbb{R}$. The template is deformed into a smooth curve $\mathcal{S} \subset \mathbb{R}^2$ embedded in 2D which is unknown. We denote as $\varphi = (\varphi_x \; \varphi_y)^\top \in C^\infty(\mathcal{T}, \mathbb{R}^2)$ the embedding that parametrizes $\mathcal{S}$ from the template. The 1D input image $\mathcal{I} \subset \mathbb{R}$ is modeled as the perspective projection of $\mathcal{S}$ that we

denote with a canonical 1D projection function Π:

$$\Pi(\mathbf{Q}) = \frac{x}{y} \quad \text{where} \quad \mathbf{Q} = (x\ y)^\top, \tag{1}$$

We assume that the image coordinates are normalized by undoing the known camera's intrinsics (the focal length and principal shift). We define $\eta \in C^\infty(\mathcal{T}, \mathbb{R})$ as the registration warp between the template and the image. We assume that $\mathcal{S}$ has no self-occlusions in $\mathfrak{I}$.

The goal of 1DSfT is to recover the embedding φ, from the warp η and the projection function Π and the fact that the curve $\mathcal{S}$ deforms isometrically. The *reprojection* constraint links the warp and the embedding through camera projection:

$$\eta = \Pi \circ \varphi \tag{2}$$

The *isometry* constraint forces the geodesic distance to be preserved between $\mathcal{T}$ and $\mathcal{S}$. Isometry is a first order differential property in φ:

$$\|\varphi'\|_2^2 = 1. \tag{3}$$

From the constraints (3) and (2) we define 1DSfT as finding the solution to:

$$\text{Find} \quad \varphi \in C^\infty(\mathcal{T}, \mathbb{R}^2) \quad \textit{s.t.} \quad \begin{cases} \eta = \Pi \circ \varphi & \text{(reprojection)} \\ \|\varphi'\|_2^2 = 1 & \text{(isometry).} \end{cases} \tag{4}$$

4. Differential Analysis

4.1. ODE Formulation

We show that the 1DSfT problem (4) is equivalent to finding the solution of a first order non-linear ODE. We first transform the reprojection constraint (2) into:

$$\varphi_y \eta = \varphi_x, \tag{5}$$

which we differentiate one time, giving:

$$\eta' \varphi_y + \eta \varphi'_y = \varphi'_x. \tag{6}$$

By substituting φ'_x from equation (6) in the isometry constraint (3) and expanding, we arrive at:

$$\left(\varphi'_y \eta\right)^2 + 2\varphi_y \varphi'_y \eta\eta' + \left(\varphi_y \eta'\right)^2 + \left(\varphi'_y\right)^2 = 1. \tag{7}$$

Equation (7) is a first-order non-linear ODE with φ_y as dependent variable. Given a solution to equation (7) the embedding φ is expressed as $\varphi = \varphi'_y \bar{\eta}$.

We use equation (7) to study 1DSfT, local stability and solution space. This leads to two important results: *i)* 1DSfT is not locally solvable exactly and *ii)* 1DSfT has a discrete number of solutions.

4.2. Local Exact Solutions

We explore whether local solutions of equation (7) exist by assuming that φ_y and φ'_y are independent variables. These are called the non-holonomic solutions [11]. Our main motivation is historical as non-holonomic solutions were first proposed in [6] for the 2DSfT problem, providing a proof of well-posedness and analytic solutions. Non-holonomic solutions are based on a relaxation of the differential dependencies and creating new equations by differentiation.

We prove the following proposition regarding the existence of non-holonomic solutions to equation (7):

Proposition 1. *The non-holonomic solution for depth φ_y in equation* (7) *is under-constrained at all orders of differentiation.*

Proof. Equation (7) gives a single constraint for the two unknowns, φ_y and φ'_y. By differentiating equation (7) we can create extra equations. Differentiating $k-1$ times we obtain a total of k equations. However, with each differentiation we introduce a new unknown. For order k we have a total of $k+1$ unknowns (*i.e.* $\varphi_y, \varphi'_y, \ldots, \varphi^{(k)}$). As a consequence we have k equations and $k+1$ unknowns and the problem is under-constrained for any orders $k > 0$. □

4.3. Solution Space

We now study the *global* solutions to 1DSfT. We first transform equation (7) using a change of variable that allows us to define the so-called *critical points*, where the normal of the embedding is collinear with sightline. Critical points are shared by groups of solutions of equation (4), constraining them to tangentially intersect in 2D. We show that the number of critical points allows us to give an upper bound on the number of solutions.

4.3.1 Change of Variable

We first define $\varepsilon = \|\bar{\eta}\|$ and thus, $\varepsilon' = \frac{1}{\varepsilon}\eta\eta'$. Introducing ε and ε' in equation (7) we have:

$$\left(\varphi'_y \varepsilon + \varphi_y \varepsilon'\right)^2 - \varphi_y^2 \varepsilon'^2 + \varphi_y^2 \eta'^2 = 1. \tag{8}$$

We then define the change of variable:

$$\theta = \varphi_y \varepsilon, \tag{9}$$

which allows us to transform equation (8) into one depending on θ and θ':

$$\theta'^2 + \xi\theta^2 = 1 \quad \text{with} \quad \xi = \frac{\eta'^2}{\varepsilon^4}. \tag{10}$$

Finally we obtain θ' from equation (10) as:

$$\theta' = \pm\sqrt{1 - \xi\theta^2}. \tag{11}$$

Given a solution to equation (11) we recover a solution of the original ODE (7) by simply inverting the change of variable of equation (9).

4.3.2 Critical Points

We now give the definition of critical points and their properties that allow us to study the space of solutions of 1DSfT.

Definition 1. *Given θ_φ a solution of equation* (11)*, $u_c \in \mathcal{T}$ is a critical point of θ_φ if $\theta'_\varphi(u_c) = 0$ or alternatively $\theta^2_\varphi(u_c)\xi(u_c) = 1$.*

Let us define the normal field of an embedding φ with the operator $\mu[\varphi]$ where:

$$\mu[\varphi] = \begin{pmatrix} -\varphi'_y & \varphi'_x \end{pmatrix}^\top. \tag{12}$$

Note that $\mu[\varphi](u)$, with $u \in \mathcal{T}$, is a unit vector when φ is isometric.

Proposition 2. *Given a solution φ to equation* (4)*, $u_c \in \mathcal{T}$ is a critical point if and only if $\mu[\varphi](u_c)^\top \dfrac{\varphi(u_c)}{\|\varphi(u_c)\|_2} = \pm 1$.*

Proof. We start by writing η' in function of φ from equation (2):

$$\eta' = \frac{\varphi'_x\varphi_y - \varphi_x\varphi'_y}{(\varphi_y)^2}. \tag{13}$$

We use equation (13) in equation (10) and equation (9) to express ξ and θ:

$$\xi = \frac{\left(\varphi'_x\varphi_y - \varphi_x\varphi'_y\right)^2}{\left(\varphi_x^2 + \varphi_y^2\right)^2} \tag{14}$$

$$\theta = \sqrt{\varphi_x^2 + \varphi_y^2}. \tag{15}$$

From definition 1 we have that if u_c is a critical point then:

$$\theta^2(u_c)\xi(u_c) = 1, \tag{16}$$

where, by using Eqs. (14), (15) and (12) we have that:

$$\begin{aligned}\theta^2(u_c)\xi(u_c) =& \frac{\left(\varphi'_x(u_c)\varphi_y(u_c) - \varphi_x(u_c)\varphi'_y(u_c)\right)^2}{\varphi_x^2(u_c) + \varphi_y^2(u_c)} \\ =& \left(\mu[\varphi](u_c)^\top \frac{\varphi(u_c)}{\|\varphi(u_c)\|_2}\right)^2.\end{aligned} \tag{17}$$

□

Proposition 2 gives a geometric interpretation of the critical points: they represent the points of the curve $\mathcal{S}$ where the normal and the optical ray are collinear.

Proposition 3. *Given φ and γ two solutions of equation* (4) *where $u_c \in \mathcal{T}$ is a critical point of both φ and γ then we have $\varphi(u_c) = \pm\gamma(u_c)$.*

Proof. If φ and γ are two solutions of equation (4) they both respect the reprojection constraint $\Pi \circ \varphi = \Pi \circ \gamma$. This property is equivalent to:

$$\exists \rho \in C^\infty(\mathbb{R}, \mathbb{R}) \quad s.t. \quad \varphi = \rho\gamma. \tag{18}$$

We define $\theta_\varphi = \epsilon\varphi_y$ and $\theta_\gamma = \epsilon\gamma_y$ which are solutions of equation (11). From equation (18) we have that $\theta_\varphi = \rho\theta_\gamma$. Now if u_c is a critical point we have from definition 1 that $\theta'_\varphi = 0$ and $\theta'_\gamma = 0$ and thus:

$$\theta^2_\varphi\xi = \rho^2\theta^2_\gamma\xi = 1 \quad \text{and} \quad \theta^2_\gamma\xi = 1. \tag{19}$$

From equation (19) we have that $\rho^2 = 1$ and thus $\varphi = \pm\gamma$. □

Proposition 4. *Given two solutions φ and γ to equation* (4)*, if $u_c \in \mathcal{T}$ is a critical point of φ and not of γ then $\|\gamma(u_c)\|^2 \leq \|\varphi(u_c)\|^2$.*

Proof. Differentiating equation (18) we have that:

$$\varphi'_x = \rho'\gamma_x + \rho\gamma'_x \quad \varphi'_y = \rho'\gamma_y + \rho\gamma'_y. \tag{20}$$

From the result of proposition 2 we have that if u_c is a critical point of φ then:

$$\frac{\left(\varphi'_x(u_c)\varphi_y(u_c) - \varphi_x(u_c)\varphi'_y(u_c)\right)^2}{\varphi_x^2(u_c) + \varphi_y^2(u_c)} = 1. \tag{21}$$

We substitute φ in equation (21) using equation (18) and equation (20) to obtain an equation with $\rho(u_c)$ and $\gamma(u_c)$:

$$\rho^2(u_c)\left(\frac{\gamma'_x(u_c)\gamma_y(u_c) - \gamma_x(u_c)\gamma'_y(u_c)}{\gamma_x^2(u_c) + \gamma_y^2(u_c)}\right)^2 = 1, \tag{22}$$

which can be expressed from equation (17) as follows:

$$\rho^2(u_c)\left(\mu[\gamma](u_c)^\top \frac{\gamma(u_c)}{\|\gamma(u_c)\|_2}\right)^2 = 1. \tag{23}$$

From equation (23) we have that $\rho^2(u_c) \geq 1$, as $\rho^2(u_c)$ is multiplied by the squared dot product of two unit vectors, which is always ≤ 1. Thanks to equation (18), we have $\|\gamma(u_c)\|^2 \leq \|\varphi(u_c)\|^2$. □

In proposition 3 we show that all solutions sharing a critical point are constrained to intersect in 2D. However in proposition 4 we show that all critical points are not necessary shared by all solutions. In fact, critical points of a solution do not propagate to solutions that are closer to the retina. We show next a way to characterize all critical points of equation (4) for all solutions.

Proposition 5. *A point $u_c \in \mathcal{T}$ is a critical point of equation* (4) *if it is a solution of the equation:*

$$2\eta(u_c)\eta'^2(u_c) - \left(1+\eta^2(u_c)\right)\eta''(u_c) = 0$$

Proof. We derive a condition on η that is valid at critical points. We first differentiate equation (10) to get the following ODE:

$$2\theta'\theta'' + \xi'\theta^2 + 2\xi\theta\theta' = 0. \tag{24}$$

We assume φ is a solution to equation (4) with $u_c \in \mathcal{T}$ a critical point. We have that $\theta_\varphi = \epsilon\varphi_y$ is a solution to equation (24) and $\theta'_\varphi(u_c) = 0$ from definition 1. We substitute θ_φ in equation (24) and evaluate the result at u_c, obtaining the following condition:

$$\xi'(u_c)\theta^2_\varphi(u_c) = 0. \tag{25}$$

As $\theta_\varphi(u_c)^2 \neq 0$, otherwise φ passes through the camera's origin at u_c, we have that $\xi'(u_c) = 0$, where:

$$\xi' = \frac{2\varepsilon^4\eta'\eta'' - 4\varepsilon^3\varepsilon'\eta'^2}{\varepsilon^8}, \tag{26}$$

from which we have that $\xi'(u_c) = 0$ is equivalent to:

$$\frac{\varepsilon^3}{\eta'}\left(\varepsilon(u_c)\eta''(u_c) - 2\varepsilon'(u_c)\eta'(u_c)\right) = 0. \tag{27}$$

By substitution of ϵ and ϵ' in terms of η and removing factors in equation (27) we have the following condition:

$$2\eta(u_c)\eta'^2(u_c) - (1+\eta^2(u_c))\eta''(u_c) = 0, \tag{28}$$

which only depends on η and its derivatives. □

Proposition 5 is important as it gives an equation for finding all critical points from the known η, without requiring to compute all solutions of equation (4). As we explain below, the number of critical points gives us a bound for the maximum number of solutions of equation (4).

4.3.3 Bounding the Number of Solutions

We use the properties of critical points given in the previous section and the Picard-Lindelöf (PL) theorem to give an upper bound on the number of solutions to 1DSfT (4). The PL theorem provides conditions for the existence and uniqueness of solutions in first-order ODEs with initial conditions. We reproduce its definition as: *Consider the following initial value problem in a general ODE with θ as dependent variable and u as independent variable,*

$$\begin{cases} \theta' = \psi(\theta, u) \\ \theta(u_0) = \theta_0. \end{cases} \tag{29}$$

If ψ is a Lipschitz continous function in θ and continous in u for all $u \in [u_0-\epsilon; u_0+\epsilon]$ with $\epsilon > 0$ then there exists a unique solution to equation (29) *in the interval $[u_0-\epsilon; u_0+\epsilon]$.*

To apply the PL theorem in equation (11) we study an open interval between two consecutive critical points u_{c_1} and u_{c_2} where the sign of θ' does not change.

Proposition 6. *Given two consecutive critical points u_{c_1} and u_{c_2} and given a solution θ_φ of equation* (11)*, the sign of θ'_φ remains constant in the interval $I = (u_{c_1}; u_{c_2})$.*

Proof. We assume that θ_φ has continuous derivatives and $\theta'_\varphi(u_{c_1}) = 0$ and $\theta'_\varphi(u_{c_2}) = 0$ by definition 1. Therefore the function θ'_φ cannot change its sign in the interval I without passing through a critical point which contradicts the fact that there are no critical points in I. □

Using proposition 6 we give the following result:

Proposition 7. *Given the open interval $I = (u_{c_1}; u_{c_2})$ between two consecutive critical points, there exist a maximum of 4 solutions of equation* (11) *in I.*

Proof. We assume a point $u_0 \in I$ and a solution θ_+ of (11) where $\theta_+(u_0) > 0$ and $\theta'_+(u_0) > 0$. From proposition 6, θ'_+ does not change sign in I and thus it is a solution of (11) taking positive sign in the square root:

$$\theta' = \sqrt{1-\xi\theta^2}. \tag{30}$$

We take partial derivatives of equation (30) to show that it is Lipschitz continous in I:

$$\frac{\partial\psi}{\partial\theta} = \frac{-\xi\theta}{\sqrt{1-\xi\theta^2}}. \tag{31}$$

As I is a finite interval and the denominator of equation (31) is never zero in I then ψ' is bounded and ψ is Lipschitz continous. We define $\epsilon > 0$ such that the interval $I_{u_0} = [u_0-\epsilon; u_0+\epsilon]$ is contained in I. Note that I_{u_0} always exists by making ϵ small enough. As a consequence, from the LP theorem we can conclude that the solution θ_+ is unique in the interval I_{u_0}. By repeating the same process for all points $u_0 \in I$ we demonstrate that the solution θ_+ is unique in I.

We repeat the same argument for a solution θ_- where $\theta_-(u_0) > 0$ and $\theta'_-(u_0) < 0$. In this case the ODE is given by $\theta' = -\sqrt{1-\xi\theta^2}$. By using the PL theorem we show that indeed if θ_- exists it is unique in the interval I. We conclude the proof by highlighting that we count also as solutions the mirrored versions of θ_+ and θ_- which gives a total of 4 possible solutions in the interval I. □

Note that from now on only positive, *i.e.* real, solutions are considered. From proposition 7 we can derive the following bound on the number of solutions, given the number of critical points.

Corollary 1. *For N critical points in $\mathcal{T}$, there are $M \leq 2^N - 1$ possible solutions to equation* (4).

Proof. Considering proposition 7, between two successive critical points there are 2 possible solutions. From proposition 3 we know that solutions intersect in the critical points. Therefore, the solutions to (4) are composed of chunks that connect at the critical points. For N critical points we have $M \leq 2^N - 1$ possible combinations. □

5. Computational Solutions

Our approach is based on the fact that one solution is needed to find the critical points and to compute the second solution. Our 1DSfT method is composed of 4 main steps, shown in figure 2:

1. **Initialization:** in this step we propose two strategies to find an initial solution. The first strategy is to assume that the sought after solution of equation (4) is infinitesimally planar. We then can use equation (33) to give a solution. The second strategy is based on the Maximum Depth Heuristic (MDH) which yields to a convex SOCP.
2. **Refinement:** we use an isometric parametrization of the solution and non-linear local optimization to refine the solution given by the previous step. This step requires an accurate initialization given in the previous step.
3. **Critical points:** we use the properties of critical points to find them in the solution given by refinement. The template $\mathcal{T}$ is then divided in intervals given by consecutive critical points where there is a maximum of 4 solutions.
4. **Finding all solutions:** we use refinement to find all solutions on each interval by forcing all different combinations of signs for θ and θ'.

5.1. Initialization

5.1.1 Non-Holonomic Analytic Solution under Infinitesimal Planarity

One way to initialize the refinement is provided by an analytical solution. We show that a special case of the 1DSfT problem can be solved locally and analytically. In this special case we assume the deformed curve $\mathcal{S}$ to be infinitesimally planar. This is equivalent to consider $\mathcal{S}$ as a succession of infinitesimal lines, *i.e.* to consider that for every $u \in \mathcal{T}$, $\varphi''(u) = \mathbf{0}$. Using the result from proposition 1 we have that by differentiation of equation (7) we find the following system with 2 unknowns and 2 equations.

$$\begin{aligned} \left(\varphi'_y\varepsilon + \varphi_y\varepsilon'\right)^2 - \varphi'^2_y\varepsilon'^2 + \varphi^2_y\eta'^2 = 1 \\ 2(\varphi'_y)^2\eta\eta' + \varphi_y\varphi'_y\left(2(\eta')^2 + \eta\eta''\right) + \varphi^2_y\eta'\eta''. \end{aligned} \quad (32)$$

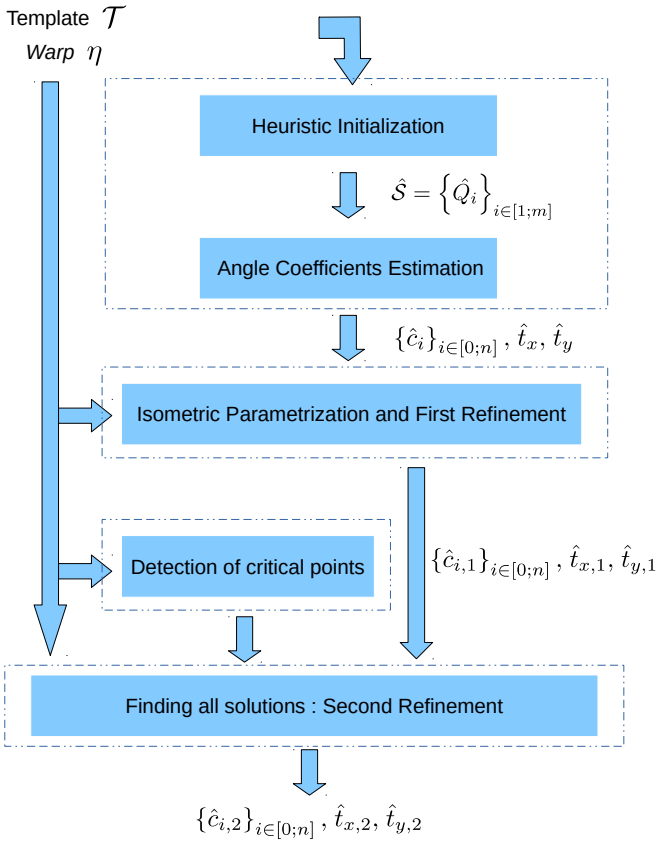

Figure 2. Proposed 1DSfT method.

By removing φ'_y from the two equations in equation (32) we have two solutions for φ_y:

$$\varphi_y = \pm\frac{2\eta'}{\sqrt{\left(-\eta''\eta + 2(\eta')^2\right)^2 + \left(-\eta''\right)^2}}. \quad (33)$$

The infinitesimal assumption can be generalized for higher orders assuming that for $u \in \mathcal{T}$, $\varphi^{(k)}(u) = \mathbf{0}$. This makes φ locally a polynomial of finite order. However, unlike infinitesimal planarity, for $k > 2$ analytical solutions cannot be found and the solution requires to solve a system of polynomials. We keep the positive solution. The first and second derivatives of the warp are computed thanks to a polynomial approximation.

5.1.2 Maximum Depth Heuristic

This isometry constraint relaxation [13] is based on three strong points. It is a second-order cone program (SOCP) optimization. This method moves the 2D points $\hat{\mathbf{Q}}_i$ along each sightline, what preserves the reprojection constraint. It maximizes the distance between the 2D points such that

they are lower or equal to the geodesic distance between the equivalent 1D points u_i in $\mathcal{T}$:

$$\left\| \hat{\mathbf{Q}}_i - \hat{\mathbf{Q}}_j \right\|_2 \leq |u_i - u_j| \,. \tag{34}$$

5.2. Isometric Parametrization and Refinement

One contribution of this work is the isometric parametrization of the embedding function. Such a parametrization is difficult to achieve for 3D objects. 1DSfT allows us to try it in a simpler setting. We assume that the template $\mathcal{T}$ is composed by m ticks with a distance l between two successive points. Instead of constraining isometry during the refinement, the embedding function is made isometric by construction, using an angle function $\alpha : \mathcal{T} \to \mathbb{R}$:

$$\forall u_i \in \mathcal{T}, \quad \varphi(u_i) = l \sum_{j=1}^{i} \begin{pmatrix} \cos\alpha(u_j) \\ \sin\alpha(u_j) \end{pmatrix} + \begin{pmatrix} t_x \\ t_y \end{pmatrix}, \tag{35}$$

with $\alpha(u_j) = \sum_{k=0}^{n} u_j^k c_k$, a n-degree polynomial. Thus, the embedding function is defined by $n+3$ parameters: shape and translation parameters, $\{c_i\}_{i\in[0;n]}$,t_x and t_y.

The refinement is performed by a nonlinear least-squares optimization on a cost function containing only the reprojection constraint.

$$\varepsilon_d(c_0, ..., c_n, t_x, t_y) = \frac{1}{m} \sum_{i=1}^{m} \left| f \frac{\varphi_x(u_i)}{\varphi_y(u_i)} - \eta(u_i) \right|^2 . \tag{36}$$

6. Experimental Results

We evaluate our methods on real and synthetic data. We use three types of relative error measurements to quantify the robustness and accuracy of our method: isometry constraint, shape and reprojection. We test against noise in the image, shape of the deformed object and number of correspondences.

6.1. Implementation Details

We use MATLAB to perform experiments with YALMIP [2] and SeDuMi 1.3 [1] to implement the MDH. We perform the first refinement by 'lsqnonlin' and the second refinement by 'fmincon' since we have to constraint the sign of θ'.

6.2. Synthetic Experiments

A perspective camera model is used and the template is normalized. To control the shape, we change the curvature of a line, *i.e.* the inverse of the radius for an arc. First, we compare the MDH (§5.1.2) and the analytical solution provided by the analytical solution (§5.1.1). The MDH is more robust to deformation since its shape error is less than 1% while the non-holonomic solution gives an average shape error of 20%.

For experiments on curvature and number of points, isometry is exactly fulfilled while reprojection is met to a very good extent. The MDH fulfills the reprojection constraint because of its formulation, but shows higher errors on the isometry since it is a relaxation and it forces points to move along the sightlines. Figure 3 shows the error made on reconstructing the 2D deformed curve as a function of the three parameters.

For curvature and number of points, an additive gaussian noise of $\sigma = 1.0$ px is added in the 1D image correspondences. That explains why the MDH presents the highest error in the figure. When curvature decreases, the ground truth curve tends to be a line and both solutions merge. In the same experiments, we observe that one refinement provides the solution near to the ground truth and the other one a second isometric solution. Finally, the angle-based parameterization in both refinements allows to overcome the errors made by the MDH, at a certain level of noise.

6.3. Real Experiments

Real data are built thanks to a 3D reconstruction of a bent paper. Figure 4 shows the one used for these experiments: we want to reconstruct the middle line shown by the cyan line in the image. Two sets of images are taken: one for the 1D image and one for the 3D reconstruction from which we can extract a 2D slice. To get the 1D image, the principal axis of the camera has to intersect the bars region. The middle row of the image is thus considered for the 1D image. We take images of size 4800×3200 px. The software Agisoft photoscan [3] is used to reconstruct the 3D scene. We construct a data set with 7 isometric deformations which are soft, without self-occlusion and performed horizontally like in figure 4.

Figure 4 shows good relative errors on shape (less than 1%) and, for all data, the 2D reconstruction results present two solutions of deformed curves. We also give an example of results that our method provides. This example illustrates well that sign of θ' changes between two solutions of equation (11) and that both solutions share the same critical points.

7. Conclusion

We have presented a theoretical study of isometric 1DSfT and its implementation. 1DSfT reveals its complexity through ODE analysis. We introduce the notion of critical points which give a bound on the solution space. We prove local exact 1DSfT solutions do not exist and that 1DSfT cannot be solved uniquely. We give methods to compute all solutions based on convex initialization followed by non-convex refinements. We also contribute in this work with an angle-based parametrization of isometric

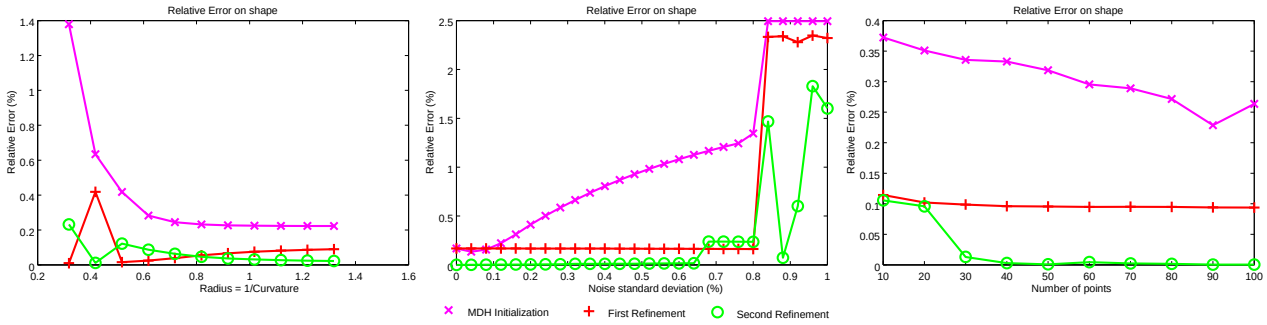

Figure 3. Synthetic data experiments. We show here the influence of three important parameters on the 1DSfT.

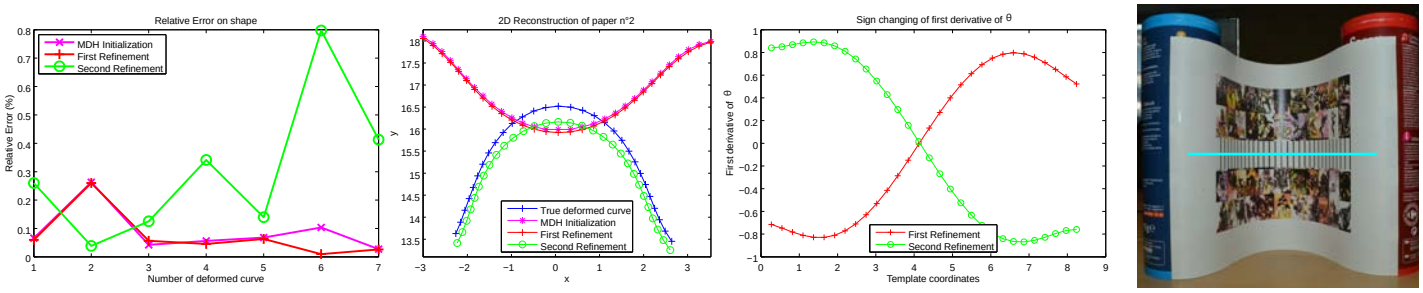

Figure 4. Real data experiments. Evaluation of the results obtained by our method - Example of results with real data - Sign changes of θ' - Image used to obtained the 1D image.

embeddings. Experiments with synthetic and real data give encouraging results, but a more thorough evaluation is needed considering complex deformation and different image conditions. Possible extensions of this work include curve-based 2DSfT and 1DSfT for more complicated slices of 3D objects.

Acknowledgements. This research has received funding from the EU's FP7 through the ERC research grant 307483 FLEXABLE.

References

[1] SeDuMi 1.3. `http://sedumi.ie.lehigh.edu`.

[2] YALMIP version 19-June-2014. `http://users.isy.liu.se/johanl/yalmip`.

[3] Agisoft PhotoScan 1.0.4, 2014.

[4] E. A. Abbott. *Flatland: A Romance of Many Dimensions*. Seely & Co., 1886.

[5] A. Bartoli. Maximizing the predictivity of smooth deformable image warps through cross-validation. *Journal of Mathematical Imaging and Vision*, 31(2-3):133–145, 2008.

[6] A. Bartoli, Y. Gérard, F. Chadebecq, and T. Collins. On template-based reconstruction from a single view: Analytical solutions and proofs of well-posedness for developable, isometric and conformal surfaces. In *CVPR*, 2012.

[7] F. Brunet, R. Hartley, and A. Bartoli. Monocular template-based 3D surface reconstruction: Convex inextensible and nonconvex isometric methods. *Computer Vision and Image Understanding*, 125:138–154, 2014.

[8] A. Chhatkuli, D. Pizarro, and A. Bartoli. Stable template-based isometric 3D reconstruction in all imaging conditions by linear least-squares. In *CVPR*, 2014.

[9] Y. Dai, H. Li, and M. He. A simple prior-free method for non-rigid structure-from-motion factorization. *International Journal of Computer Vision*, 107(2):101–122, 2014.

[10] A. Del Bue, X. Llado, and L. Agapito. Non-rigid metric shape and motion recovery from uncalibrated images using priors. In *CVPR*, 2006.

[11] Y. Eliashberg and N. M. Mishachev. *Introduction to the h-Principle*. Number Grad. Stud. Math. 48. American Mathematical Society, 2002.

[12] A. Malti, R. Hartley, A. Bartoli, and J. Kim. Monocular template-based 3D reconstruction of extensible surfaces with local linear elasticity. In *CVPR*, 2013.

[13] M. Perriollat, R. Hartley, and A. Bartoli. Monocular template-based reconstruction of inextensible surfaces. In *BMVC*, 2008.

[14] M. Salzmann and P. Fua. Linear local models for monocular reconstruction of deformable surfaces. *IEEE Transactions on Pattern Analysis and Machine Intelligence*, 33(5):931–944, 2011.